In-Flight Performance of the TES Loop Heat Pipe Heat Rejection System – Seven Years In Space

Jose I. Rodriguez and Arthur Na-Nakornpanom
Jet Propulsion Laboratory/ California Institute of Technology, Pasadena, California, USA 91109

The Tropospheric Emission Spectrometer (TES) instrument heat rejection system has been operating in space for nearly 8 years since launched on NASA's EOS Aura Spacecraft. The instrument is an infrared imaging fourier transform spectrometer with spectral coverage of 3.2 to 15.4 microns. The loop heat pipe (LHP) based heat rejection system manages all of the instrument components waste heat including the two mechanical cryocoolers and their drive electronics. Five propylene LHPs collect and transport the instrument waste heat to the near room temperature nadir viewing radiators. During the early months of the mission, ice contamination of the cryogenic surfaces including the focal planes led to increased cryocooler loads and the need for periodic decontamination cycles. Focal plane decontamination cycles require power cycling both cryocoolers which also requires the two cryocooler LHPs to turn off and on during each cycle. To date, the cryocooler LHPs have undergone 24 start-ups in orbit successfully. This paper reports on the TES cryocooler loop heat pipe based heat rejection system performance. After a brief overview of the instrument thermal design, the paper presents detailed data on the highly successful space operation of the loop heat pipes since instrument turn-on in 2004. The data shows that the steady-state and transient operation of the LHPs has not changed since 2004 and shows consistent and predictable performance. The LHP based heat rejection system has provided a nearly constant heat rejection heat sink for all of its equipment which has led to exceptional overall instrument performance with world class science.

Nomenclature

AFT	=	Allowable Flight Temperature
CCHP	=	constant conductance heat pipe
EOS	=	Earth Observing System
FPA	=	focal plane array
FPOMA	=	focal plane optical mechanical assembly
IEM	=	Integrated Electronics Module
IR	=	Infrared
JPL	=	Jet Propulsion Laboratory
LEO	=	Low Earth Orbit
LHP	=	Loop Heat Pipe
NASA	=	National Aeronautics and Space Administration
NGST	=	Northrop Grumman Space Technology
OB	=	optical bench
PCS	=	pointing and control subsystem
SAE	=	Society of Automotive Engineers
TES	=	Tropospheric Emission Spectrometer

I. Introduction

THE Tropospheric Emission Spectrometer (TES) instrument, designed and built by the Jet Propulsion Laboratory for NASA, has been operating successfully in space since launched onboard the Earth Observing System (EOS) Aura spacecraft on July 15, 2004. The EOS Aura project is managed by NASA's Goddard Space Flight Center and is the third and final mission of NASA's EOS Program. The EOS Aura observatory hosts a suite of scientific instruments designed to make the most comprehensive measurements ever undertaken of atmospheric trace gases.

Aura's orbit provides complete coverage of the globe with a 16 day repeat cycle. TES measurements are being used to determine local atmospheric temperature and humidity profiles, local surface temperatures, and local surface reflectance and emittance. The observations are also being used to study volcanic emissions for hazard mitigation, indications of the chemical state of the magma, eruption prediction, and quantification of the role of volcanoes as sources of atmospheric aerosols. A detailed description of TES and its science capabilities is found in Refs. 1-2.

TES is a cryogenic instrument with a two-stage passive cooler to cool the interferometer optical bench (OB) and two pulse tube cryocoolers for cooling the focal plane arrays (FPAs). A detailed description of the instrument is found in Refs. 3-7. The instrument is shown in Fig. 1 in its flight configuration with the Earth shade deployed while Fig. 2 shows the stowed launch configuration.

The instrument thermal control system makes use of a combination of constant conductance heat pipes (CCHPs) and loop heat pipes (LHPs) to manage the instrument power dissipation. TES utilizes five propylene LHPs and six ammonia CCHPs for waste heat management. The CCHPs are used to collect distributed waste heat from the power dissipating components and transfer the heat to the LHP evaporators. The cryocooler compressors with their high heat flux thermal interface do not require the use of CCHPs. The LHP evaporators are mounted directly to the compressor thermal interface. The LHPs transport this waste heat to the instrument nadir radiator panels. The condenser of each LHP is bonded to the underside of the nadir radiator panels.

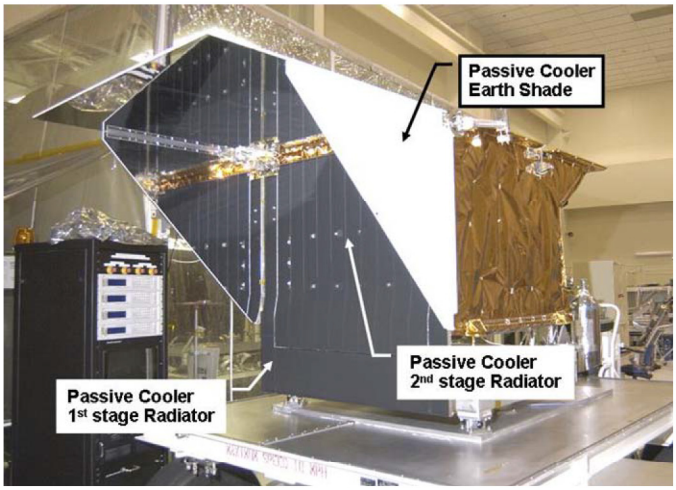

Figure 1. TES instrument with Earth shade deployed.

Figure 2. TES instrument with Earth shade stowed.

In a 2008 paper (Ref. 6), the in-space performance of the heat rejection system was published with the focus on the initial start-up behavior of all LHPs and early performance. The current paper presents LHP performance data to date, 4 years later, with a focus on the transient behavior of the cryocooler LHPs during shut-down and start-up for every power cycle event of the cryocoolers. This undesirable consequence of ice contamination on the focal planes has lead to a fortunate circumstance allowing the detailed study of the transient behavior of LHPs in a space application. Sufficient engineering telemetry is available to assess the performance of these devices as they age in a low Earth orbit (LEO) space environment.

II. Instrument Description

The heart of the TES instrument is four FPAs located in two separate focal-plane opto-mechanical assemblies (FPOMAs) cooled to 65K by a pair of single-stage pulse tube cryocoolers. The interferometer optics including the FPOMA housings are maintained near 180K by means of a passive cooler. The passive cooler first stage cools the thermal shield surrounding the optics bench and intercepts parasitic heat leaks from the surrounding environment near 300K whereas the second stage cools the interferometer optics. The instrument envelope is 1.4 m by 1.3 m by 1.35 m with the Earth shade stowed and 3.04 m by 1.3 m by 1.35 m with the Earth shade deployed. The allocated mass and average operating power is 355kg and 334W, respectively.

Figure 3. Cryocooler B LHP condenser configuration.

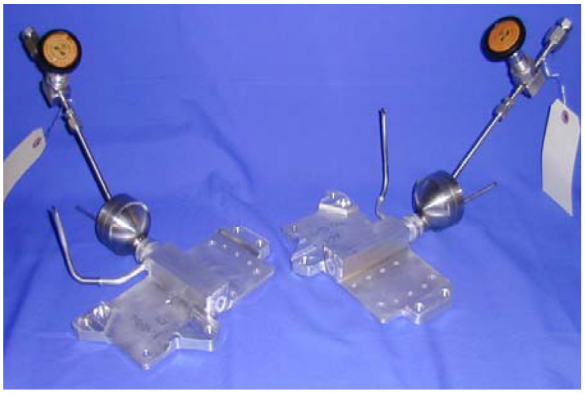

Figure 4. Cryocooler A and B LHP evaporator configuration.

A. Heat Rejection System Thermal Design

The selection of LHPs for use on the TES instrument solved three key thermal control problems: 1) LHPs permit the thermal decoupling of the equipment to radiators in survival mode with a small amount of heater power, 2) they enable the packaging of equipment within the instrument envelope and meet the cable length and routing requirements as well as the structural design constraints, and 3) they allow thermal vacuum testing of instrument in horizontal and vertical orientations at instrument and spacecraft-level. The implementation of LHPs provided the required design space to meet all the thermal, electrical, structural, and mechanical configuration requirements. A detailed description of the TES instrument thermal control system is available in Refs. 3-4. The cryocooler B LHP condenser and evaporators are shown in Figs. 3-4. The cryocooler LHP assembly with radiators is shown in Fig. 5. The evaporator designs are identical, whereas the condensers are not as shown in Fig. 5.

In survival mode the spacecraft rotates about its velocity vector which results in a fairly cold space environment for the nadir radiators which experience orbital temperature variations between -96 to -71ºC with an orbit period of 98 minutes. Ammonia if used would pose a serious risk because it freezes at -78ºC and it could potentially result in rupturing the thin LHP condenser lines attached to the radiators if it thaws with two frozen plugs on either side. Propylene with a freezing point of -180ºC and flight heritage was selected instead. The heat transport capacity of propylene is lower compared to ammonia by about 60-80%. In this application, the performance penalty for using propylene was acceptable with minimum impact to the thermal control system.

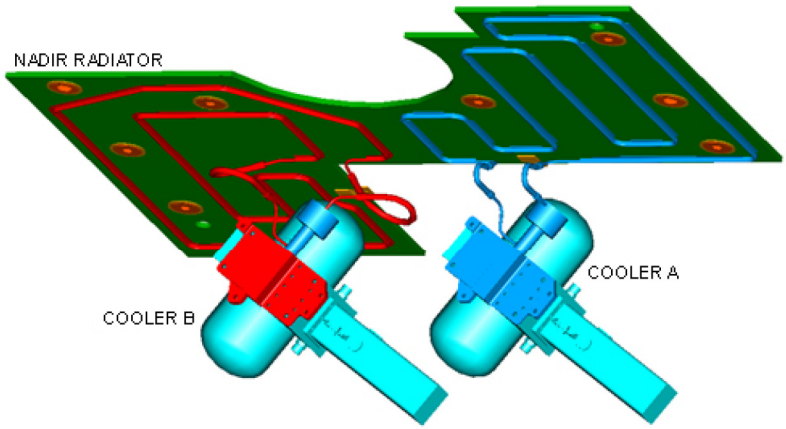

Figure 5. Cryocooler LHPs and radiator configurations.

Thermal control for the near room temperature zone uses a combination of CCHPs and LHP systems to transport and manage the equipment power dissipation. The temperature control requirements with average power dissipation are listed in Table 1. The nadir radiators are composed of three separate thermally isolated panels; 1) cryocooler radiator for rejecting waste heat from both cryocooler compressors, 2) electronics radiator for rejecting waste heat from the integrated electronics module (IEM) and cryocooler electronics and 3) signal chain radiator to reject heat from signal chain and laser head electronics. The evaporators are attached to the power dissipation components with a bolted interface and the condensers are bonded to the radiator panels. All LHPs make use of flexible sections for the vapor and liquid return lines at both transitions to the evaporator and condenser (Fig. 3). This facilitates integration of the LHPs to the equipment.

Start-up and survival heaters were added to all five LHPs to assure reliable start-ups on equipment power up and shut-downs when transitioning to survival mode when the instrument is commanded off. The start-up heaters were placed on the evaporator bodies and include two bi-metallic thermostats in series which close on temperature rise. A

single heater was used at each evaporator body. The thermostat setpoints were chosen such that the start-up heater is energized near the operating allowable fligh temperature (AFT) high limit and shuts down 3-4ºC below this limit. This approach provides a backup to a condition where the LHP fails to start-up on its own after the equipment is powered on. The shut-down heater is a Kapton film heater with wire wound elements and was bonded to the LHP compensation chamber. The shut-down heater circuit does not include a thermostat, but is powered continuously by means of a relay which closes when the instrument is commanded off. This assures the LHP compensation chamber remains a few degrees C warmer while in survival mode assuring the LHP remains off. Each compensation chamber has a single shut-down heater. Fig. 6 shows the cryocooler LHP condenser layout within the radiator. Note, the cooler A radiator temperature sensor is located near the vapor line inlet, whereas the cooler B is near the liquid return line. The configuration for the cooler B LHP condenser is such that the radiator temperature measured for this LHP is more of an average temperature between the inlet vapor and liquid return lines. Cooler A radiator temperature sensor measures the vapor line inlet temperature. Note that because of the proximity of the two radiator temperature sensors and location of vapor line inlets some thermal cross-talk is expected. Fig. 7 shows the cryocooler compressor with the LHP attached in the flight configuration.

In survival mode, when the instrument is powered off, the effective radiator sink temperature drops from -30ºC to -100ºC and a limited amount of power is available to maintain equipment temperatures within the AFT non-operating limits. While in this mode, the LHPs are shut-off to prevent heat transport from the equipment to the cold radiator panels. This is a key thermal control requirement needed to meet the stringent spacecraft survival power allocation defined as 30% of the nominal instrument operating power.

	Allowable Flight Temperatures (°C)[1]				
	Non-operat	Operating			
	Survival	Orbit Variation	Gradient	Design	Average Power (W)
IEM[2]	-25/50	5		0/50	100.8
Signal Chain Electronics	-25/50	5		0/35	28.7
Cryocooler Electronics	-25/50	5		0/50	16.0/ea
Laser Head Electronics	-25/50			0/35	5.9
Cryocooler Compressor	-25/50			0/35	43.5/ea
Translator Actuator Encoder	-25/50			-10/40	4.25
Roller Bearings	230/300K			230/250K	n.a.
Optical Bench-Optics Housing	165/300K	±2 K	20K	177 ± 2K	n.a.
Filter Wheel	65/300K			65/90K	n.a.
Filter Wheel Actuator	-50/50			-33/50	0.76
Detectors	64/300K	±1 K		65±1K	0.03/ea
Detector Pre-Amplifier	230/300K			230/250K	0.9/ea
Earth Shade Mechanism	-50/50			-43/30	n.a.
Gimbal Roll Motor	-25/50	5[2]		-10/50	n.a.
PCS Motor/Encoder	-25/50			-10/50	0.6
PCS Mirror	-25/50			-10/50	n.a.
Radiometric Calibrator	-25/50			0/50	3.5

1. All temperatures in degrees C unless otherwise noted
2. Peak-to-peak orbit variation

Table 1. Allowable flight temperature requirements and average equipment power dissipation.

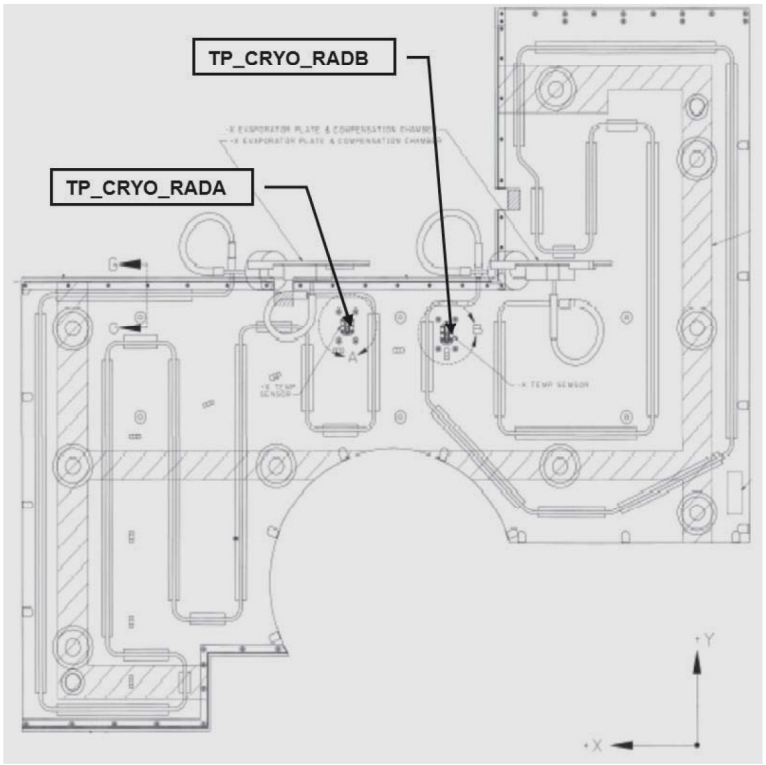

Figure 6. Cryocooler LHP condenser layout on radiator with flight radiator temperature sensor locations shown: A) TP_CRYO_RADA for cooler A LHP, and B) TP_CRYO_RADB for cooler B LHP.

The use of LHPs on TES facilitated the mechanical configuration layout for the entire instrument and allowed the thermal decoupling of the components from the radiators in survival mode.

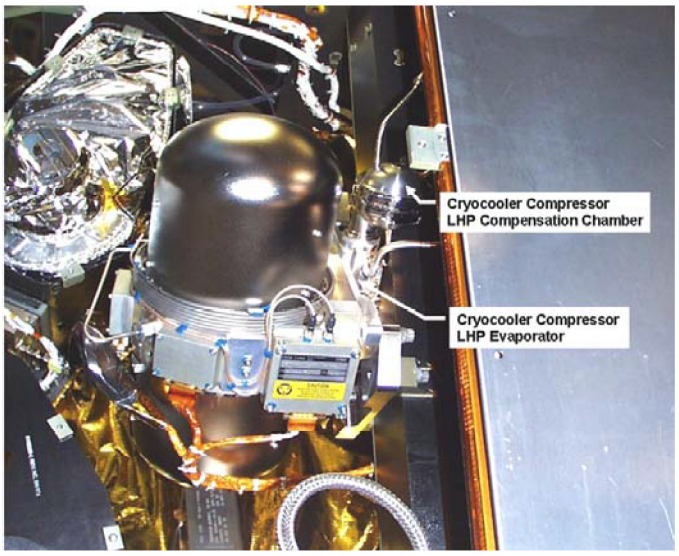

Figure 7. Cryocooler compressor with LHP evaporator.

B. Heat Rejection System Initial On-orbit Performance

After a successful launch, the Aura spacecraft was put in survival mode to checkout critical subsystems and then transitioned to nadir pointing on day 2. The initial 36-day commissioning of the instrument proved successful with all subsystems working as expected. All the LHPs powered on successfully with the exception of the cooler electronics one. The cooler electronics LHP failed to start when powered up as expected from ground testing experience (Ref. 10). After powering on the cooler electronics, its temperature increased from -2ºC to 35ºC initially and after about 1 day it stabilized at 31ºC. This was expected behavior and was acceptable because the AFT operating high limit is 35ºC. It was expected that cooler electronics power would increase due to increased heat loads on the coolers, consequently, it was very likely that the 35ºC AFT limit would have been violated during the mission lifetime without an operating LHP. There are two cooler electronics chassis each with a power dissipation of only 16W each and with a mass of 6.6kg each. Under these conditions, the initial rate of temperature increase for the LHP evaporator is only 3.1 C/hr with one cooler electronics on and 5.7 C/hr with both powered on. This is the lowest rate of temperature increase of all five LHP evaporators, and therefore, this behavior was expected (Refs. 8-11). On day 34, both cooler electronics were initialized and both compressors were powered on the same day. In this case, the radiator average temperature varied from -16ºC to 0ºC while the other radiators typically varied from -35ºC to 20ºC prior to LHP start-up. The cooler electronics shares the same radiator panel with the IEM, and therefore, sees a warmer radiator prior to start-up. The cooler electronics LHP started operating inexplicably 133 days after powered on. An investigation showed no indications of spacecraft or instrument events including maneuvers to trigger the start-up. After start-up, the cooler electronics LHP evaporator temperature decreased from 31ºC to the expected temperature near 6ºC. Ref. 6 provides additional details on this event with a more indepth discussion.

C. Cryocooler LHP Long-Term On-orbit Performance

The instrument began nominal operations on day 36 (mid-August 2004) with operational focal planes at 65K. Only 14 days after

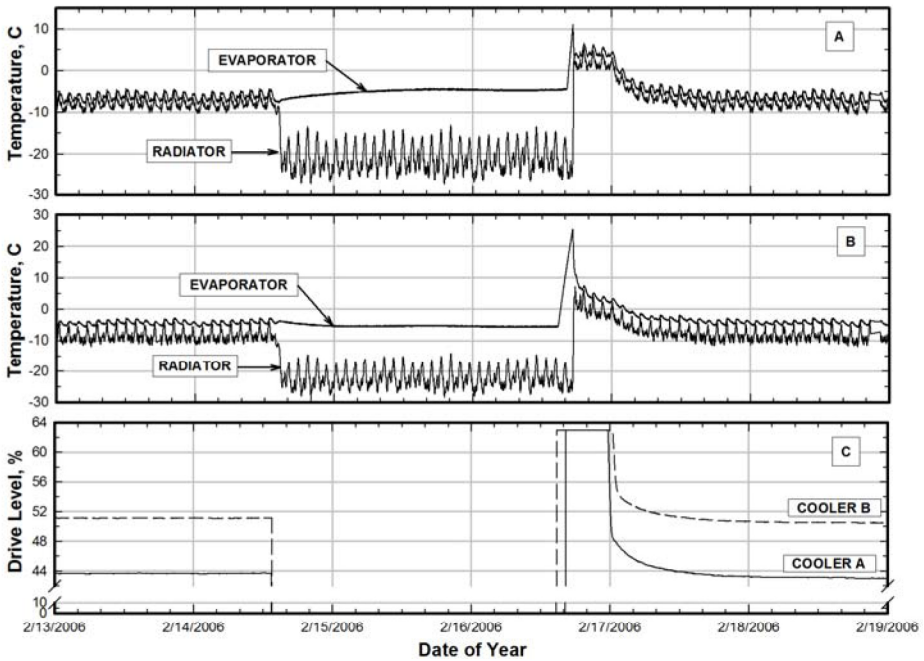

Figure 8. Decontamination cycle 15 - Cryocooler A and B LHP shutdown and startup, A) Cooler A LHP, B) Cooler B LHP, C) Cooler A and B drive levels.

the start of nominal science operations, the instrument underwent its first detector decontamination cycle. Although the radiation parasitic heat loads on the coolers increased due to the ice buildup of cryogenic surfaces, there was sufficient power margin for the coolers to continue to provide a 63K coldtip temperature needed for cooling the focal planes to 65K. Both compressors were commanded to zero stroke and the cooler electronics remained on to continue to monitor the cooler status. After 2 days of outgassing, the focal plane decontamination heater was shutdown and the coolers were powered on to cool the detector to their operating temperature. This decontamination sequence has been repeated a total of 23 times to date. Ref. 5 contains a detailed description of the cooler subsystem initial on-orbit performance.

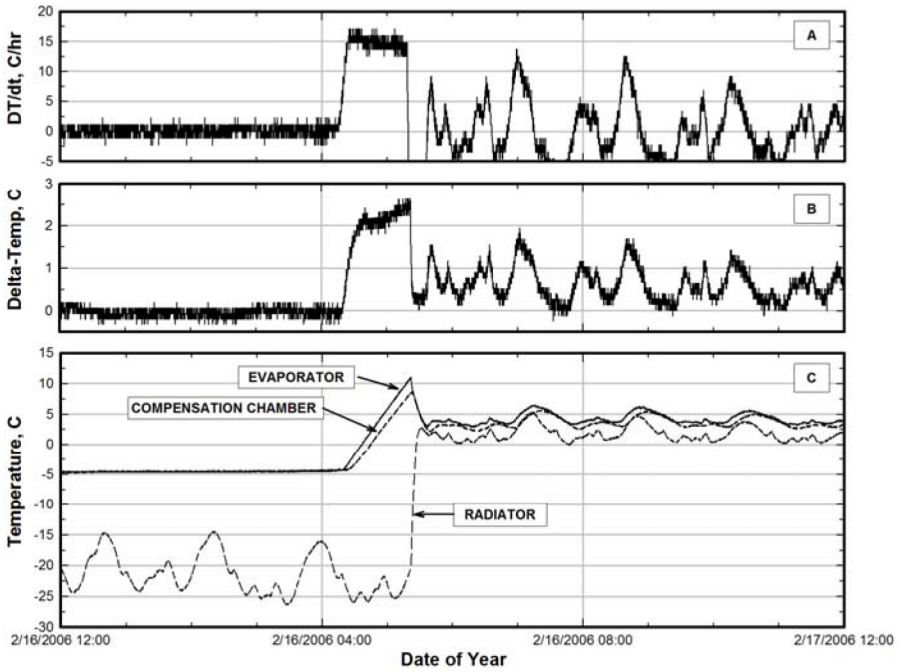

Figure 9. Decontamination cycle 15 - Cryocooler A LHP startup, A) Evaporator temperature rate of change, B) Superheat, C) Evaporator, compensation chamber and associated radiator.

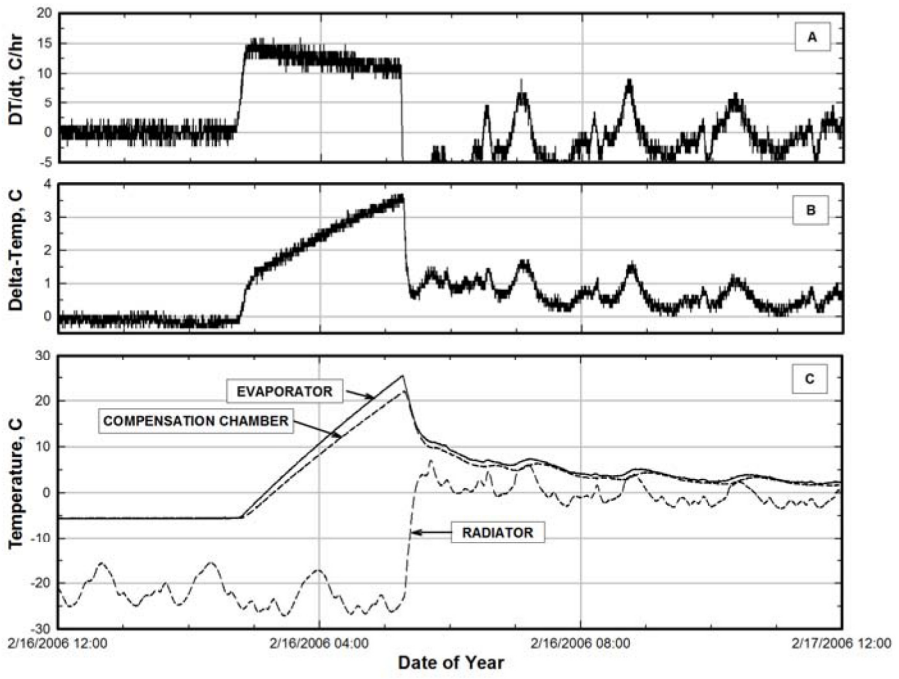

Figure 10. Decontamination cycle 15 - Cryocooler B LHP startup, A) Evaporator temperature rate of change, B) Superheat, C) Evaporator, compensation chamber and associated radiator.

All 23 LHP shutdown and start-up events have been successful; however, there are important differences that will be discussed herein. The transient behavior of decontamination cycle 15 is very typical of most of the decontamination events and is shown in Figs. 8-10. Fig. 8 shows a 6-day data set for the entire decontamination event including sufficient data to show a full recovery after the event. The cryocooler drive level plot clearly indicates when the coolers were turned off and on. When the coolers are powered on, they operate at the maximum allowed drive level of 63% and after they achieve the target coldtip operating temperature of ~63K the drive level decreases to nearly 44% for cooler A and 51% for cooler B. This difference in steady state drive levels is due to differences in cooler efficiency and total coldtip heat loads. The evaporators of both LHPs operate at higher temperatures when the coolers are operating at 63% drive level, as expected, and reach the orbital quasi-

steady state temperatures after the coolers reach their steady-state drive levels as shown in Fig. 8. Fig. 9 shows the LHP evaporator and compensation chamber temperatures for the cooler A LHP, whereas, Fig. 10 shows the cooler B LHP temperatures. The evaporator temperature rate of change and the temperature difference between the compensation chamber and evaporator are also shown in Figs 9-10. This data clearly shows the behavior for a successful LHP start-up. The temperature difference between evaporator and compensation chamber represents the superheat available for start-up and will be refered to as "superheat" in the remainder of the paper. Cooler A LHP started up with a ~2.5ºC superheat whereas cooler B LHP required a larger ~3.5ºC superheat. The evaporator temperature rate of change is approximately the same for both LHPs. As expected, the evaporator temperature rate of change peaks near the beginning of cooler power on and decreases slightly with time until LHP start-up.

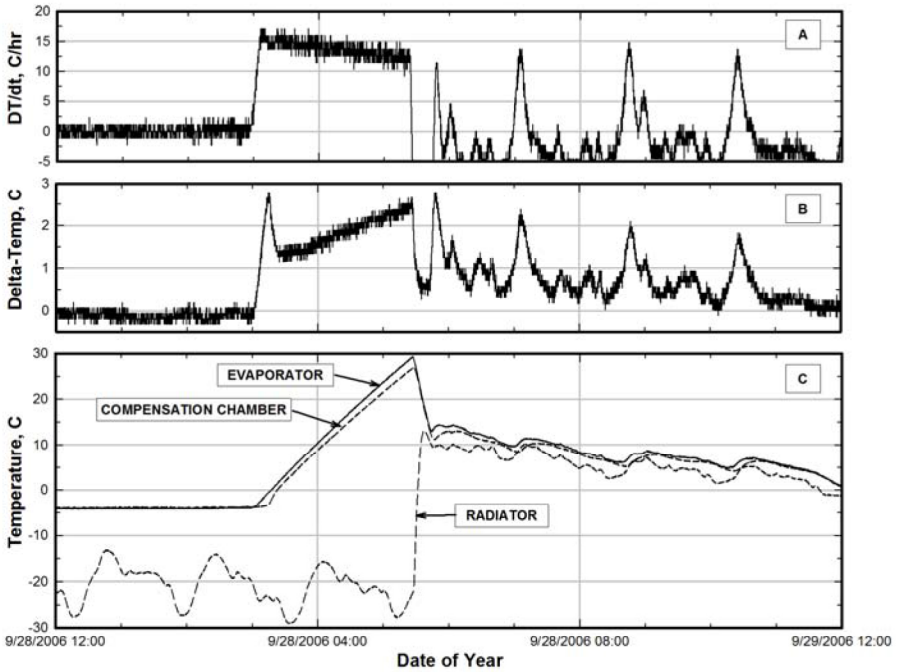

Figure 11. Decontamination cycle 16 - Cryocooler A LHP startup, A) Evaporator temperature rate of change, B) Superheat, C) Evaporator, compensation chamber and associated radiator.

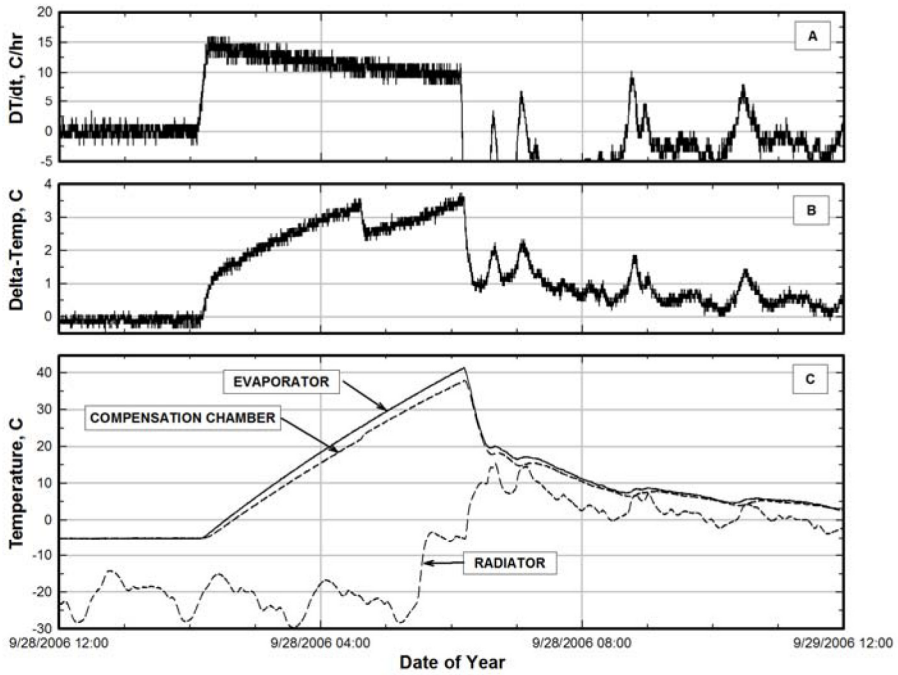

Figure 12. Decontamination cycle 16 - Cryocooler B LHP startup, A) Evaporator temperature rate of change, B) Superheat, C) Evaporator, compensation chamber and associated radiator.

The temperature data of all 23 decontamination events has been analyzed and a summary of the results is presented in Figs 11-14. Three decontamination events for cooler A LHP show a peculiar spike in the temperature difference between evaporator and compensation chamber at cooler power-on. This had no apparent effect in the start-up process for the LHP and has only been observed with this LHP. Similarly, cooler B LHP has demonstrated the behavior shown in Fig. 12 on five occasions and cooler A LHP only once. The cause of this behavior is not known. The effect of these five events on cooler B LHP caused the evaporator temperature to trigger the power on of the start-up heater. After the evaporator temperature reached 41ºC, the 15W start-up heater was energized and

almost imediately the LHP started operating as shown in Fig. 12. The only event, with similar behavior for cooler A LHP was on initial cooler power on, however, in this case it did not require the start-up heater to power on. In fact, the cooler A LHP has never required the use of the start-up heater. These sudden drops in superheat result in delaying the LHP start-up which eventually leads to the LHP requiring the aid of the start-up heater for a successful start-up. The cause of the sudden superheat drop is not known, but it is clearly not an indication of start-up because the vapor-line line temperature indicated by the radiator temperature is not affected as shown in Fig. 12. During a successful start-up as shown in Figs. 11-12, the vapor line temperature increases to the saturation temperature while the liquid line temperature drops.

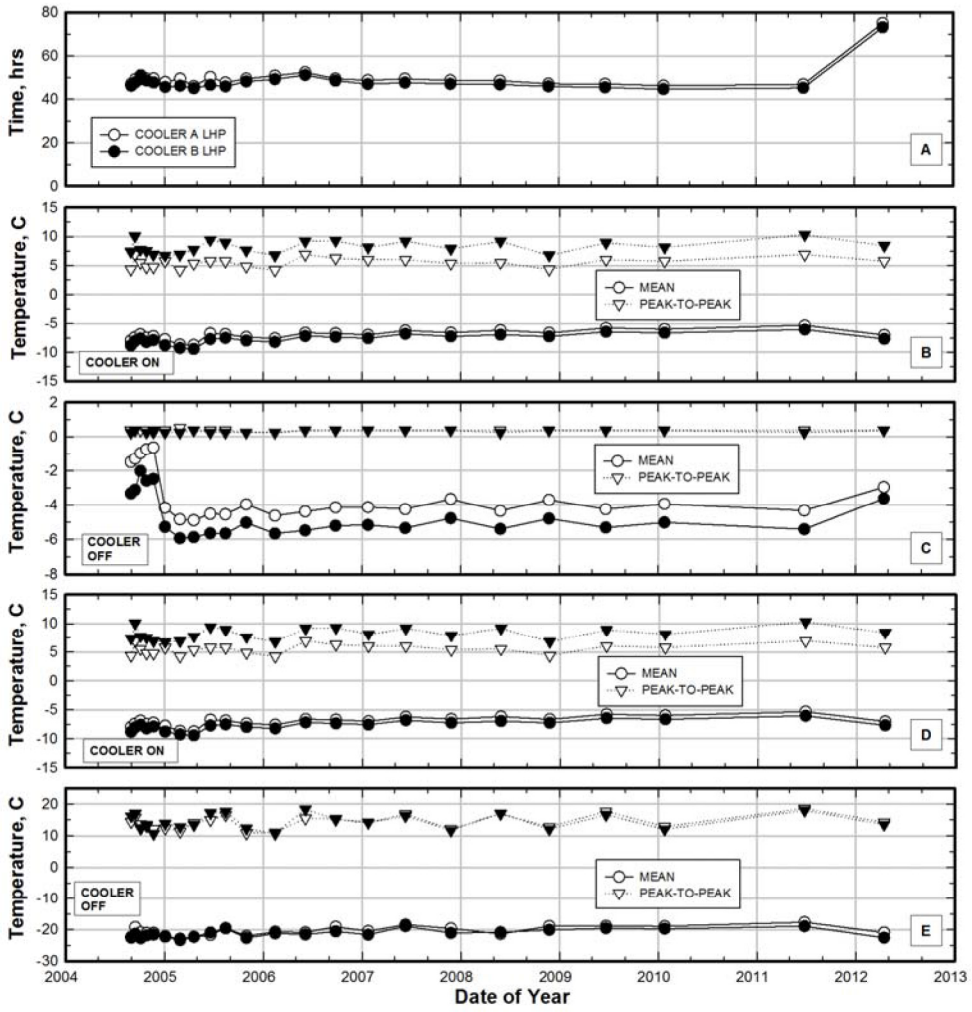

Figure 13. On-orbit data summary for entire mission duration: A) Cryocooler off time duration, B) Evaporator temperature prior to cooler shut-down, C) Evaporator temperature after cooler shut-down, D) Radiator temperature prior to cooler shut-down, E) Radiator temperature after cooler shut-down. Note, the filled-in symbols refer to cooler B LHP.

A summary of all the on-orbit data collected for the decontamination events is presented in Figs. 13-14. Fig. 13 shows data for the cryocooler off-time, LHP evaporator and radiator mean and peak-to-peak temperatures both for prior to the cooler shutdown and during the off period prior to start-up. In all cases, with the exception of the most recent decontamination cycle, the coolers were off for about 2 days with cooler B powered on first and then cooler A about 1-2 hours later. Both LHPs with separate condensers share the same radiator, and therefore, there is some thermal cross-talk evident in the flight data. The evaporator temperatures of both LHPs are nearly the same prior to cooler power off but differ by about 1.5ºC when both coolers are off. The radiator orbital temperature variation for the cooler B LHP when operating appears to be about 4ºC peak-to-peak higher which in turn causes the evaporator temperature to vary by the same amount. When both LHPs are off, the radiator mean and orbital peak-to-peak are essentially identical. It also appears that the mean radiator temperature has increased slightly by about 2ºC from the beginning of the mission. This can be attributed to a slight degration of the white paint on the radiator which is not unexpected for almost 8 years of flight operations with about 15% of the orbit with sun exposure on the nadir radiators. The evaporator temperature after cooler power off was higher by about 4ºC for the first 6 decontamination events as shown in Fig. 13. This was the results of a warmer instrument structure a consequence of a non-operating cooler electronics LHP.

In all other cases, cooler A LHP consistently started operating with a lower superheat than cooler B LHP. The cooler A LHP superheat for startup was 2.54±0.40ºC, whereas cooler B LHP was 3.58±0.23ºC, a difference of about 1ºC (see Fig. 14). The data also shows that the cooler A LHP evaporator temperature rate of change is slightly higher than cooler B LHP. After power on, both coolers operate at 63% drive level and therefore, dissipate the same amount of waste heat for about 6-9 hours which is the time needed for the coolers to reach their steady state operating coldtip temperature. Due to this behavior cooler A LHP consistently started operating within a shorter period of time, after cooler power on, than cooler B LHP as shown in Fig. 14. The five decontamination events for cooler B LHP where the start-up heater was triggered is clearly evident in Fig. 14 with peak evaporator temperatures of 41ºC. In all cases, this event was triggered in 249 minutes from cooler power on. In the most recent decontamination cycle from April 2012, the coolers were unpowered for a total of 3 days rather than the typical 2 days. This change did not appear to impact the behavior of the LHP start-up sequence. In this case, the cooler B LHP required the use of the start-up heater to power on due to the same sudden drop in superheat observed previously.

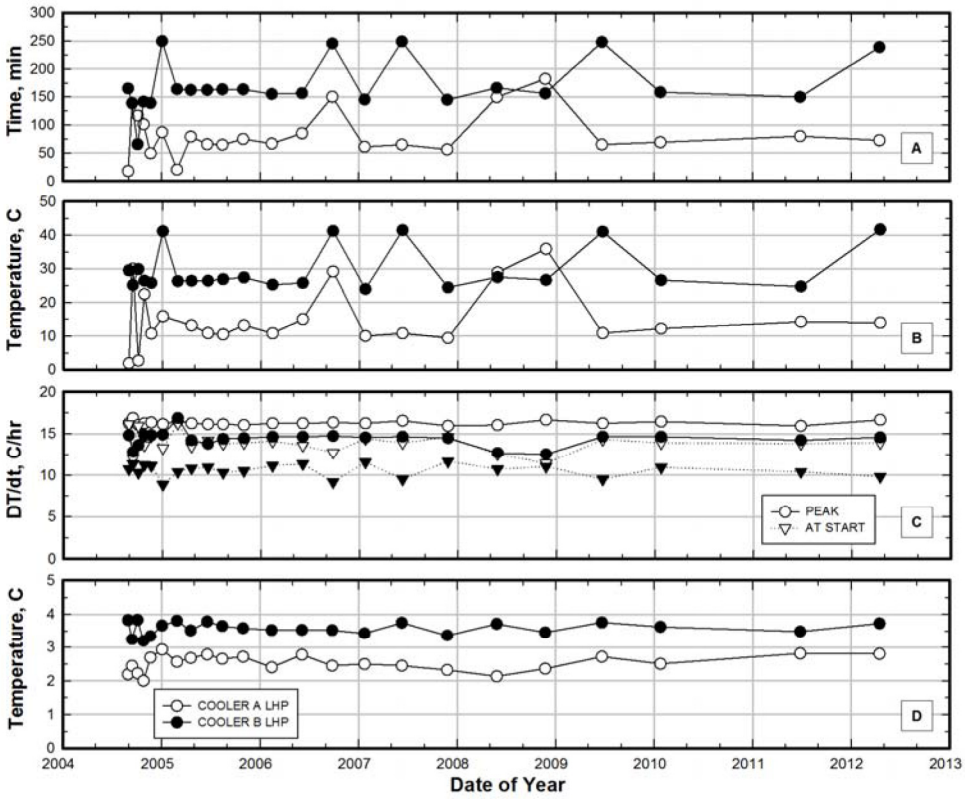

Figure 14. On-orbit data summary for LHP start conditions: A) LHP start time after cooler power on, B) Maximum LHP evaporator temperature at start-up, C) Evaporator temperature rate of change at start-up and peak from cooler power on, D) Superheat at start-up. Note the filled-in symbols refer to cooler B LHP.

III. Conclusion

The TES LHP based heat rejection system development activity was key to the success of the TES instrument development and in particular the LHP technology application solved key technical issues central to the overall instrument performance. The use of the LHPs in space has provided important data and lessons learned along with important operational factors to consider for future applications. To date, the overall thermal control system approach, has demonstrated very good thermal performance. In summary, the TES instrument mechanisms are showing signs of aging, as the instrument approaches nearly 8 years of operations, and undoubtedly will continue to degrade; however, the LHP based heat rejection system is performing to specification and shows no indications of degradation. The thermal control system is expected to continue to operate well for the remainder of the mission.

Acknowledgments

The authors would like to thank the support of the TES flight operations teams from JPL and the NASA's Goddard Space Flight Center as well as the TES Project office. Special thanks to Michael Nikitkin and Dave Feenan from ATK Space Systems (formely Dynatherm Corp.) who supplied the CCHPs and LHPs.

The work described in this paper was carried out at the Jet Propulsion Laboratory California Institute of Technology, Northrup Gumman Aerospace Systems, ATK Space Systems, and Utah State University Space Dynamic Lab; it was sponsored by the NASA EOS TES Project Office through an agreement with the National Aeronautics and Space Administration.

References

[1]Glavich, T.A., and Beer, R., "Tropospheric Emission Spectrometer for the Earth Observing System," *SPIE Proceedings*, Vol. 1540, Bellingham, Washington, July 1991.

[2]Beer, R., "TES on the Aura Mission: Scientific Objectives, Measurements, and Analysis Overview," *IEEE Transactions on Geoscience and Remote Sensing,* Vol. 44, No. 5, May 2006.

[3]Rodriguez, J.I., "Thermal Design of the Tropospheric Emission Spectrometer Instrument," *30th SAE* Paper 2000-01-2274, July 2000.

[4]Collins, S.A., Rodriguez, J.I., and Ross, R.G., "TES Cryocooler System Design and Development," *Advances in Cryogenic Engineering*, Vol 47B, Amer. Inst. of Physics, NY, 2002, pp. 1053-1060.

[5]Rodriguez, J.I., Collins, S.A., Na-Nakormpanom, A., Johnson, D.L., "On-Orbit Performance of the TES Pulse Tube Coolers and Instrument - A First Year in Space", *Advances in Cryogenic Engineering*, Vol 51B, Amer. Inst. of Physics, NY, 2006, pp. 1937-1944.

[6]Rodriguez, J.I., Na-Nakornpanom, A., Rivera, J.G., Mireles, V., and Tseng, H., "On-Orbit Performance of the TES Instrument – Three Years in Space," *38th SAE* Paper No. 2008-01-2118, July 2008.

[7]Rodriguez, J.I., Na-Nakornpanom, A., "On-Orbit Performance of the TES Cryocooler System and the Instrument – Six Years in Space," *Advances in Cryogenic Engineering,* Vol. 54b, Plenum Press, New York , NY, 2011, pp. 000-000.

[8]Rodriguez, J. I., and Na-Nakornpanom, A., "Investigation of Transient Temperature Oscillations of a Propylene Loop Heat Pipe," *SAE* Paper No. 2001-01-2235.

[9]Ku, J., "Operating Characteristics of Loop Heat Pipes," *SAE* Paper No. 1999-01-2007, July 1999.

[10]Rodriguez, J.I., Pauken, M. and Na-Nakorpanom, A., "Transient Characterization of a Propylene Loop Heat Pipe during Startup and Shutdown," 30th *SAE* Paper No. 2000-01-2408, July 2000.

[11]Pauken, M. and Rodriguez, J.I., "Performance Characterization and Model Verification of a Loop Heat Pipe," 30th *SAE* Paper No. 2000-01-2317, July 2000.